Structure of the Functional Fragment of Auxilin Required for Catalytic Uncoating of Clathrin-Coated Vesicles‡

James M. Gruschus,[§,||] Chae J. Han,[||,⊥] Tsvika Greener,[⊥] James A. Ferretti,[§] Lois E. Greene,[⊥] and Evan Eisenberg*[,⊥]

Laboratory of Biophysical Chemistry and Laboratory of Cell Biology, National Heart, Lung, and Blood Institute, National Institutes of Health, Bethesda, Maryland 20892

Received August 18, 2003; Revised Manuscript Received December 20, 2003

ABSTRACT: The three-dimensional structure of the C-terminal 20 kDa portion of auxilin, which consists of the clathrin binding region and the C-terminal J-domain, has been determined by NMR. Auxilin is an Hsp40 family protein that catalytically supports the uncoating of clathrin-coated vesicles through recruitment of Hsc70 in an ATP hydrolysis-driven process. This 20 kDa auxilin construct contains the minimal sequential region required to uncoat clathrin-coated vesicles catalytically. The tertiary structure consists of six helices, where the first three are unique to auxilin and believed to be important in the catalytic uncoating of clathrin. The last three helices correspond to the canonical J-domain of Hsp40 proteins. The first helix, helix 1, which contains a conserved FEDLL motif believed to be necessary for clathrin binding, is transient and not packed against the rest of the structure. Helix 1 is joined to helix 2 by a flexible linker. Helix 2 packs loosely against the J-domain surface, whereas helix 3 packs tightly and makes critical contributions to the J-domain core. A long insert loop, also unique to the auxilin J-domain, is seen between helix 4 and helix 5. Comparison with a previously reported structure of auxilin containing only helices 3−6 shows a significant difference in the invariant HPD segment of the J-domain. The region where helix 1 is located corresponds to the expected region of the unstructured G/F-rich domain seen in DnaJ, i.e., the canonical N-terminal J-domain protein. In contrast, the location of helix 1 differs from the substrate binding regions of two other Hsp40 proteins, *Escherichia coli* Hsc20 and viral large T antigen. The variety of biological functions performed by Hsp40 proteins such as auxilin, as well as the observed differences in the structure and function of their substrate binding regions, supports the notion that Hsp40 proteins act as target-specific adaptors that recruit their more general Hsp70 partners to specific biological roles.

The Hsc70[1] class of molecular chaperones is involved in numerous processes in the cell, including assisting in the folding of newly synthesized proteins, preventing denaturation and aggregation, and in assembling and disassembling protein complexes (*1*). There is considerable evidence that substrates rapidly bind to and dissociate from Hsc70, which is an ATPase, in the ATP-bound form, while substrates are tightly bound to Hsc70 in the ADP-bound form, dissociating very slowly until ATP rebinds (*2*). In most of its functions, Hsc70 requires the action of a class of cofactor proteins known as Hsp40, or, equivalently, J-domain proteins (*3*). These proteins contain a 70-amino acid residue J-domain with an invariant HPD motif that specifically binds to Hsc70. This HPD motif is essential for activity both *in vitro* and *in vivo* (*4*−*6*). Various studies have shown that J-domain proteins such as Hsp40 act by presenting protein substrates to Hsc70 (*1*, *7*). The J-domain protein binds the protein substrate, transfers it to the Hsc70−ATP molecule, and finally induces rapid hydrolysis of ATP to ADP, thereby locking the protein substrate onto the Hsc70−ADP molecule.

One of the best characterized functions of Hsc70 that requires a specific J-domain protein is the uncoating by Hsc70 of clathrin-coated vesicles in an ATP-dependent reaction (*8*−*10*). Both *in vitro* and *in vivo*, this uncoating activity of Hsc70 requires catalytic amounts of the 100 kDa, nerve-specific J-domain protein auxilin or the related widely expressed protein GAK (auxilin 2). Auxilin has beeen shown to be required for uncoating in yeast, *Caenorhabditis elegans*, and in mammalian systems (*11*−*13*). Auxilin was originally identified as a minor clathrin assembly protein, since it also induces clathrin to polymerize into clathrin baskets (*14*). Mammalian auxilin has a C-terminal J-domain, a clathrin binding region, and an N-terminal tensin segment of unknown function. In addition to these domains, GAK has an N-terminal ARK kinase domain whose function is also not understood but which is a functional kinase (*9*) and can phosphorylate the medium chains of AP2 and AP1 (*10*). Biochemical characterization of the interaction of Hsc70 and auxilin with clathrin-coated vesicles or clathrin baskets has

‡ The coordinates have been deposited as Protein Data Bank entry 1N4C.

* To whom correspondence should be addressed: Laboratory of Cell Biology, Building 50, Rm 2525, National Institutes of Health, Bethesda, MD 20892-0301. Telephone: (301) 469-1001. Fax: (301) 402-1519. E-mail: eisenbee@nhlbi.nih.gov.

§ Laboratory of Biophysical Chemistry.

|| These authors contributed equally to this work.

⊥ Laboratory of Cell Biology.

[1] Abbreviations: Hsp70, heat shock protein 70 (kilodaltons); Hsc70, heat shock cognate 70 (kilodaltons); Hsp40, heat shock protein 40 (kilodaltons); Hsc66, heat shock cognate 66 (kilodaltons); Hsc20, heat shock cognate 20 (kilodaltons); GAK, cyclin G-associated kinase; NOESY, nuclear Overhauser effect spectroscopy; HSQC, heteronuclear single-quantum coherence; HMQC, heteronuclear multiple-quantum coherence; TOCSY, total correlation spectroscopy; rms, root-mean-square; SV40, simian virus 40; Rb, retinoblastoma; AP, assembly protein.

10.1021/bi0354740
Published on Web 02/24/2004

suggested that, during the uncoating reaction, auxilin first binds to a clathrin triskelion on the clathrin basket, inducing the binding of three Hsc70−ATP molecules to the clathrin triskelion (*15*, *16*). Auxilin catalyzes the rapid hydrolysis of the Hsc70−ATP molecule to the Hsc70−ADP molecule, causing the clathrin triskelion to dissociate from the clathrin basket. Finally, auxilin detaches from the dissociated clathrin−Hsc70 complex and then binds to another triskelion in the clathrin basket, thus acting catalytically. On the other hand, Hsc70 acts stoichiometrically since, unlike auxilin (*17*), it forms a stable complex with the dissociated clathrin triskelions even in the presence of ATP (*16*). In its ability to induce catalytically the binding of Hsc70 to clathrin baskets, as well as in its ability to catalyze hydrolysis of ATP to ADP leading to formation of a stable clathrin−Hsc70 complex, auxilin acts as a typical J-domain protein. However, other J-domain homologues cannot substitute for auxilin in supporting uncoating of clathrin baskets by Hsc70, probably because the clathrin-binding domain of auxilin is unique in the J-domain family of proteins (*18*).

To determine how J-domain proteins function, it is critical to determine structures of J-domain proteins that present different substrates to Hsc70. A number of structural studies have been carried out on isolated J-domains, including a very recent study on the J-domain of auxilin, and their tertiary structures have been found to be similar (*19*). However, only with structures of proteins containing both a J-domain and a functioning substrate binding site is it possible to determine the relationship between these two domains and possibly their relationship to Hsc70 as well. The structure of a complete 20 kDa *Escherichia coli* J-domain protein that presents the iron−sulfur cluster assembly protein (IscU) to a specific *E. coli* Hsc70 protein (Hsc66) has been determined, and this structure suggests a rather rigid relationship between the substrate binding site and the J-domain of Hsc20 (*20*). The structure of the N-terminal J-domain of SV40 large T antigen, bound to its substrate, Rb tumor suppressor, has also been determined, but relatively little detailed information about how this J-domain functions or indeed whether it even interacts with Hsc70 is available (*21*). The structure of the J-domain from the *E. coli* Hsp40 homologue DnaJ has been determined in both the absence (*22*, *23*) and presence of the G/F-rich domain (*24*, *25*); however, the G/F-rich domain was unstructured, and its role in substrate interaction is not entirely clear (*25*). Auxilin, one of the best characterized of the J-domain proteins with regard to its function (*8*), would, of course, be an excellent J-domain protein to analyze structurally. Unfortunately, auxilin has not yet been crystallized and is too large for its structure to be determined by NMR, as is the 60 kDa recombinant fragment of auxilin lacking the tensin domain that has been shown to have full uncoating activity *in vitro*. However, we have recently found that the clathrin binding domain of auxilin has two subdomains, an N-terminal clathrin-binding domain that appears to be mainly involved in clathrin polymerization and a C-terminal subdomain containing the FEDLL sequence that is required for auxilin to act catalytically (*18*). A 20 kDa (182-amino acid residue) recombinant C-terminal fragment of auxilin (Aux-C20) that retains this subdomain also retains the key activities of intact auxilin (*18*, *26*). Although it is not able to induce polymerization of clathrin and binds more weakly to clathrin baskets than intact auxilin, Aux-C20 catalytically supports uncoating of clathrin baskets by Hsc70 (*18*). Therefore, in the study presented here we undertook a multidimensional heteronuclear NMR study to determine the structure of Aux-C20.

Our results suggest that J-domain protein substrate binding domains and their relationship to their respective J-domains appear to be individually adapated to their specific substrates. Helix 1 of Aux-C20, which contains the FEDLL region that presumably interacts with the distal or proximal domain of the clathrin heavy chain (*27*), is found in the expected location of the unstructured G/F-rich domain of DnaJ. However, while *E. coli* DnaJ, like many other J-domain proteins, binds weakly to Hsc70 but strongly activates its ATPase activity in the absence of substrate (*28*), auxilin binds strongly to Hsc70 and negligibly activates the Hsc70 ATPase activity in the absence of clathrin (*17*). Even larger differences are observed between the substrate binding domains of Aux-C20 and the *E. coli* Hsc20 J-domain protein; the substrate binding domain of the latter appears to be rigidly related to its J-domain (*8*, *20*), while helix 1 of Aux-C20 is flexibly related to its J-domain. Finally, the large T antigen J-domain and its substrate binding domain have orientations completely different from each other and from the respective domains of Aux-C20. Therefore, our results suggest that the substrate binding domain of each J-domain protein may be specifically tailored to its particular substrate, bringing its substrate into the correct orientation relative to the Hsc70−ATP molecule. This enables the substrate to be transferred from the J-domain protein to Hsc70 while at the same time the Hsc70 ATPase activity is activated and substrate is then trapped on the Hsc70−ADP molecule.

EXPERIMENTAL PROCEDURES

Sample Preparation. Bovine auxilin was truncated to give the 20 kDa C-terminal recombinant protein Aux-C20. Aux-C20 was expressed as a glutathione *S*-transferase (GST) fusion protein by being cloned into the pGEX 6P-1 vector (Amersham Biosciences). The ^{15}N-labeled and ^{15}N- and ^{13}C-labeled (Martek, minimal media) fusion proteins were typically prepared from 1.5 L. The cells were lysed and centrifuged, and the supernatant was then added to glutathione resin (Amersham Biosciences) at a ratio of 20 mL of protein supernatant per 5 mL of resin. The protein resin mixture was then rotated for 4 h at 4 °C. The resin was then spun, and the immobilized protein was washed three times with 300 mM KCl and 50 mM Tris (pH 7.5), followed by two washes with cleavage buffer. Then 750 units of Precission protease (Amersham Biosciences) was added and the resin rotated overnight at 4 °C. The eluant from three washes of the column was combined and applied to a DEAE column (5 mL) equilibrated in cleavage buffer which removed minor contaminants. The cleaved protein was further purified on a benzamidine−Sepharose 6 column (Amersham Biosciences) to remove any residual protease. From 1 L of cells, we obtained 10 mg of protein that was greater than 98% pure when analyzed by NMR spectroscopy. The first eight residues of Aux-C20 are from the GST fusion protein, and the remaining 174 residues are the final 174 residues of bovine auxilin (residues 737−910).

Four 1.5 mM Aux-C20 samples were prepared, one labeled with ^{15}N and one labeled with both ^{13}C and ^{15}N, at pH 7.0

in 25 mM phosphate buffer, and one labeled with ^{15}N and one labeled with both ^{13}C and ^{15}N, at pH 4.5 with 60 mM NaCl, all in a 90% H_2O/10% D_2O mixture with 5 mM 16D-EDTA. The sample lifetime was limited to 1−2 weeks; the gradual appearance of additional sharp peaks in the NMR spectra (at both pH values) indicated significant proteolytic degradation, which was verified by SDS−PAGE analyses of the samples.

NMR Experiments and Chemical Shift Assignment. All spectra were recorded on a Bruker 600 MHz DRX spectrometer, except where noted, at 300 K and at both pH values, except where noted. For the doubly labeled samples, CbCaCONH (42* × 35* × 512*, f_1 at 6172.8 Hz, f_2 at 1577.3 Hz, and f_3 at 8992.8 Hz) and CbCaNH (40* × 38* × 512*, f_1 at 5952.4 Hz, f_2 at 1577.3 Hz, and f_3 at 7183.9 Hz) (*29*) spectra were collected, as well as a short constant time (2.7 ms) ^{13}C-edited NOESY-HSQC (t_{mix} = 100 ms, 64* × 32* × 512*, f_1 at 6001.5 Hz, f_2 at 7462.7 Hz, and f_3 at 7788.2 Hz) (*30*) spectrum in the aliphatic region (^{13}C carrier at 56 ppm) with water flip back (*31*) and sensitivity enhancement (*32*) and a ^{13}C-edited NOESY-HMQC (t_{mix} = 100 ms, 96* × 46 × 512*, f_1 at 6001.5 Hz, f_2 at 6640.1 Hz, and f_3 at 7788.2 Hz) (*49*) spectrum in the aromatic region (^{13}C carrier at 125 ppm) with water flip back (*33*) WATERGATE water suppression (*34*). For the ^{15}N singly labeled sample at pH 7.0, a three-dimensional (3D) ^{15}N-edited NOESY-HSQC (t_{mix} = 80 ms, 96* × 60 × 768*, f_1 at 6001.5 Hz, f_2 at 1733.4 Hz, and f_3 at 8333.3 Hz) (*33*) spectrum with water flip back was collected, while for the pH 4.5 sample, the same experiment was performed on a Bruker 800 MHz DMX spectrometer (t_{mix} = 80 ms, 140* × 40 × 768*, f_1 at 8800.9 Hz, f_2 at 2311.1 Hz, and f_3 at 11 061.9 Hz). A ^{15}N-edited ^1H TOCSY (t_{mix} = 60 ms, 96* × 64 × 768*, f_1 at 6001.5 Hz, f_2 at 1733.4 Hz, and f_3 at 8333.3 Hz) (*50*) spectrum was collected for the pH 7.0 sample. Chemical shift assignments and preliminary secondary structural analysis have been reported previously (*35*).

Structural Restraint Determination. Normalized NOE peak intensities were used to derive distance restraints for structure calculation. Distance versus peak intensity log−log calibrations were performed for the spectra collected for the pH 4.5 samples, which include the 800 MHz ^{15}N-edited NOESY spectrum. Only nonoverlapping cross-peaks having undistorted, nonoverlapping diagonal peaks for normalization were used in the calibrations. For the ^{15}N NOESY spectrum, cross-peak intensities from clearly α-helical segments of the structure were fit to the corresponding standard α-helical distances along with intra-side chain tryptophan $H^{\epsilon 1}$ cross-peaks and corresponding distances. Similarly, for the aliphatic region ^{13}C NOESY spectrum, α-helical cross-peaks along with geminal methylene cross-peaks were used with the corresponding distances. For the aromatic region ^{13}C NOESY spectrum, tryptophan intra-side chain, phenylalanine H^{ζ} intra-side chain, and histidine intra-side chain cross-peak intensities and corresponding distances were used. The resulting exponents from the log−log fits were −4.4 for the ^{15}N NOESY spectrum, −4.4 for the aliphatic ^{13}C NOESY spectrum, and −4.3 for the aromatic ^{13}C NOESY spectrum. That the exponent results are so similar is probably coincidence; similar calibrations on other proteins have yielded more variable results (*36*). Because of spin diffusion and molecular vibrations, empirically calibrated exponents have magnitudes that are smaller than the theoretical NOE limit of −6 (*37*). In all three fits, all the cross-peak intensities were never more than a factor of 3 above and below the fitted average. For this reason, the upper and lower bounds for the distance restraints were calculated assuming a variation of a factor of 3 in intensity above and below the measured cross-peak intensity. Backbone ϕ and ψ torsional angle restraints were obtained using TALOS (*38*) using ^{13}C α- and β-resonances supplemented by α-proton and amide nitrogen and proton resonances. The ϕ and ψ restraint ranges were taken to be 4 times the uncertainty range in the TALOS output file.

Determination of the Auxilin Structure. The structure of Aux-C20 was generated using X-PLOR version 3.851 (A. Brunger, Yale University, New Haven, CT). After generation of several preliminary ensembles of structures, to check and make additional assignments and to optimize the X-PLOR parameter settings, a set of 200 structures was generated using the standard "dg_sub_embed" (backbone embedding) routine. Simulated annealing was then performed using the standard "dgsa" routine with 30 000 steps at an initial temperature of 10 000 K, followed by 10 000 cooling steps. Floating chirality was employed (*39*), with the relatively high temperature allowing sufficient prochiral sampling. Additional molecular dynamics refinement was performed on the structures using the standard "refine" routine, cooling the structures from a starting temperature of 5000 K in 25 000 steps. From the 200 refined structures, the 20 structures with the lowest X-PLOR energies were chosen for the final refinement steps. During the first stage of the refinement, both NOE restraints and experimental dihedral restraints had force constant magnitudes of 200 kcal/Å^2 and 200 kcal/rad^2, respectively, and the van der Waals repel parameter was set to 0.75 for the minimizations, while in the final refinement steps, these constants were changed to 30 kcal/Å^2 for the NOE restraints, 100 kcal/rad^2 for the dihedral restraints, and 0.8 for the repel parameter. The "sum" averaging and "square" potential options were used for the NOE restraints throughout.

In the final refinement steps, experimental restraints were carefully examined for systematic violations in the 20 structures, usually due to spin diffusion cross-peaks or a failure to account for additional degenerate resonances, and the corresponding restraints were removed or adjusted accordingly. In individual structures with local regions of nonsystematically violated restraints, typically coordinate randomization was performed in the local area and additional low-temperature (200 K) refinement performed on the structure. For the final structures, 5000 steps of minimization were performed.

Binding and ATPase Assays. Clathrin baskets, Hsc70, AP180, and auxilin were made as described previously (*18*). Binding of Aux-C20 to clathrin−AP180 baskets was assessed by mixing varying concentrations of the auxilin fragment with baskets and determining the amount bound after centrifugation in a TL-100 ultracentrifuge at 400000*g* for 6 min. ATPase activity was measured at pH 6.0 and 25 °C using [γ-^{32}P]ATP as described in ref *7*. The buffer consisted of 25 mM KCl, 10 mM ammonium sulfate, 2 mM $MgCl_2$, 1 mM dithiothreitol, and 20 mM imidazole at pH 7.0 (or 20 mM MES at pH 6).

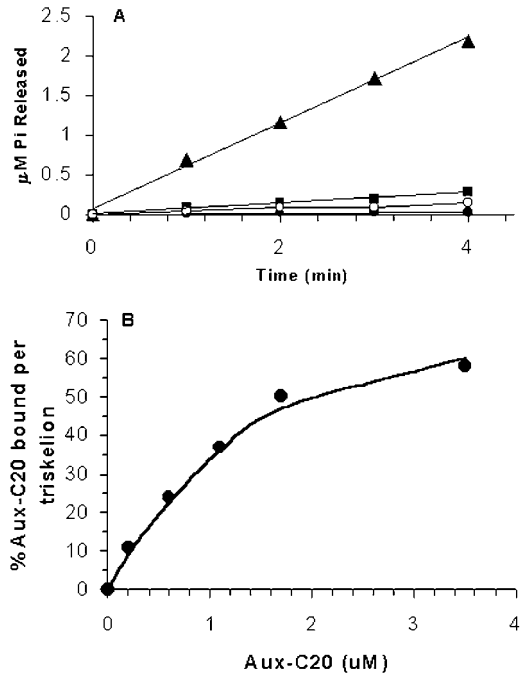

FIGURE 1: (A) Activation of Hsc70 ATPase activity by clathrin baskets at pH 6.0 by Aux-C20. The ATPase activity was measured at 25 °C using 0.6 μM Hsc70 alone (●), 0.6 μM Hsc70 with 0.6 μM Aux-C20 (■), 0.6 μM Hsc70 with 0.6 μM clathrin baskets (○), and 0.6 μM Hsc70, 0.6 μM Aux-C20, and 0.6 μM clathrin baskets (▲). (B) Binding of Aux-C20 to clathrin−AP180 baskets at pH 7.0. Varying concentrations of Aux-C20 were added to 2.5 μM clathrin baskets polymerized with the assembly protein AP180. The amount of AuxC-20 bound was determined after sedimentation and quantified from SDS gels of the supernatant. All concentrations of clathrin are expressed in terms of clathrin triskelions.

RESULTS

We previously showed that Aux-C20 catalytically supports the uncoating of clathrin baskets by Hsc70 (*18*). Panels A and B of Figure 1 show that Aux-C20 retains two other key properties of auxilin. First, at pH 6 it strongly activates the ATPase activity of Hsc70 in the presence but not in the absence of clathrin baskets, and second, it binds relatively strongly to clathrin baskets at pH 7, although it is not able to induce clathrin polymerization. Therefore, in many of its key properties, Aux-C20 is functionally quite similar to intact auxilin.

The Aux-C20 structure consists of six helices, with helix 1 starting at residue 778 of auxilin. The statistics for the structure determination using the NMR-derived restraints are given in Table 1, and a secondary structure and sequence comparison is given in Figure 2. The first three helices are unique to auxilin, and the last three correspond to the canonical J-domain structure. The initial 48 residues of Aux-C20 are unstructured (*27*). The resonances of helix 1 have broader, stronger NOESY cross-peaks than the adjacent unstructured residues, and include 15 $i-i+3$ (residues three positions apart in sequence) cross-peaks and five $i-i+4$ cross-peaks. Such cross-peaks are not seen in the adjacent stretches, and they are typical of α-helical secondary structure. The ^{13}C chemical shifts for helix 1 are more typical of random coil, however, indicating transient secondary structure (*35*, *40*). No long-range NOE cross-peaks were detected for helix 1, which is joined to helix 2 by a flexible, 13-residue linker. Helix 2 is loosely packed against helices 3 and 6, while helix 3 packs tightly with the last three helices, contributing to the hydrophobic core of the J-domain. Figure 3 shows the three-dimensional structure for the final five helices. The packing of the last four helices superficially resembles a four-helix bundle, except that helices 4 and 5 run parallel to each other, rather than antiparallel, and helix 4 is considerably shorter and less parallel to the other three helices. A long insert loop between helices 4 and 5, with well-defined structure and contributing many hydrophobic core residues, is another unique feature of the auxilin J-domain (*19*, *35*).

Table 1: Aux-C20 NMR Structure Statistics

backbone rmsd for residues 798−910 (Å)[a]	1.15
all heavy atom rmsd (Å)	1.60
backbone rmsd for residues 814−905 (Å)[b]	0.30
all heavy atom rmsd (Å)	0.76
average NOE restraint violation (2810) (Å)[c]	0.040
intra (766) (Å)[c]	0.048
sequential (854) (Å)[c]	0.041
medium-range (686) (Å)[c]	0.031
long-range (504) (Å)[c]	0.036
average $\phi-\psi$ dihedral restraint violation (144) (deg)[c]	0.71
rmsd from idealized covalent geometry	
bonds (Å)	0.0036
angles (deg)	0.43
improper dihedrals (deg)	0.30
Ramachandran plot (%)[d]	
residues 729−910	62, 34, 4, 0
residues 798−910	79, 20, 1, 0

[a] The first 69 residues are primarily random coil, except for helix 1. [b] Helices 3−6, excluding helix 2 and C-terminal residues. [c] Number of restraints in parentheses. [d] The percentages correspond to most favorable, additionally allowed, generously allowed, and disallowed regions of the Ramachandran plot.

No structurally significant differences were seen in chemical shifts or NOESY cross-peak patterns at the two pH values (4.5 and 7.0), except for D876 (of the J-domain invariant HPD sequence) and R828. The backbone amide chemical shifts of both these residues become narrower and shift downfield at the higher pH. The NOESY cross-peaks to the side chain $C^{\delta 2}$ and $C^{\epsilon 1}$ attached protons of H874 strongly restrict its conformation such that the $N^{\delta 1}$ atom is within hydrogen bonding distance of the backbone amide of D876, and position its ring such that it packs against the proline ring. A hydrogen bond to the side chain of H874 in the solution structure would explain the exceptionally downfield-shifted D876 amide resonance of 11.25 ppm at pH 7, due to not only the hydrogen bond but also the histidine ring current. At pH 4.5, the broader appearance of the upfield-shifted amide resonance is likely due to exchange between positively charged and neutral or hydrogen-bonded forms of the histidine side chain. The reason for the change in the amide resonance of R828 is not clear. This arginine is quite distant (25 Å) from D876.

DISCUSSION

The structure of Aux-C20, the minimal fragment of auxilin necessary for catalytically uncoating clathrin-coated vesicles, consists of six helices in its unbound form. Helix 1, with the conserved FEDLL motif known to interact with clathrin (*27*), does not pack against the remaining five helices and is joined by a flexible linker to helix 2, while helix 2 makes only weak contacts with the remaining helices. The last four

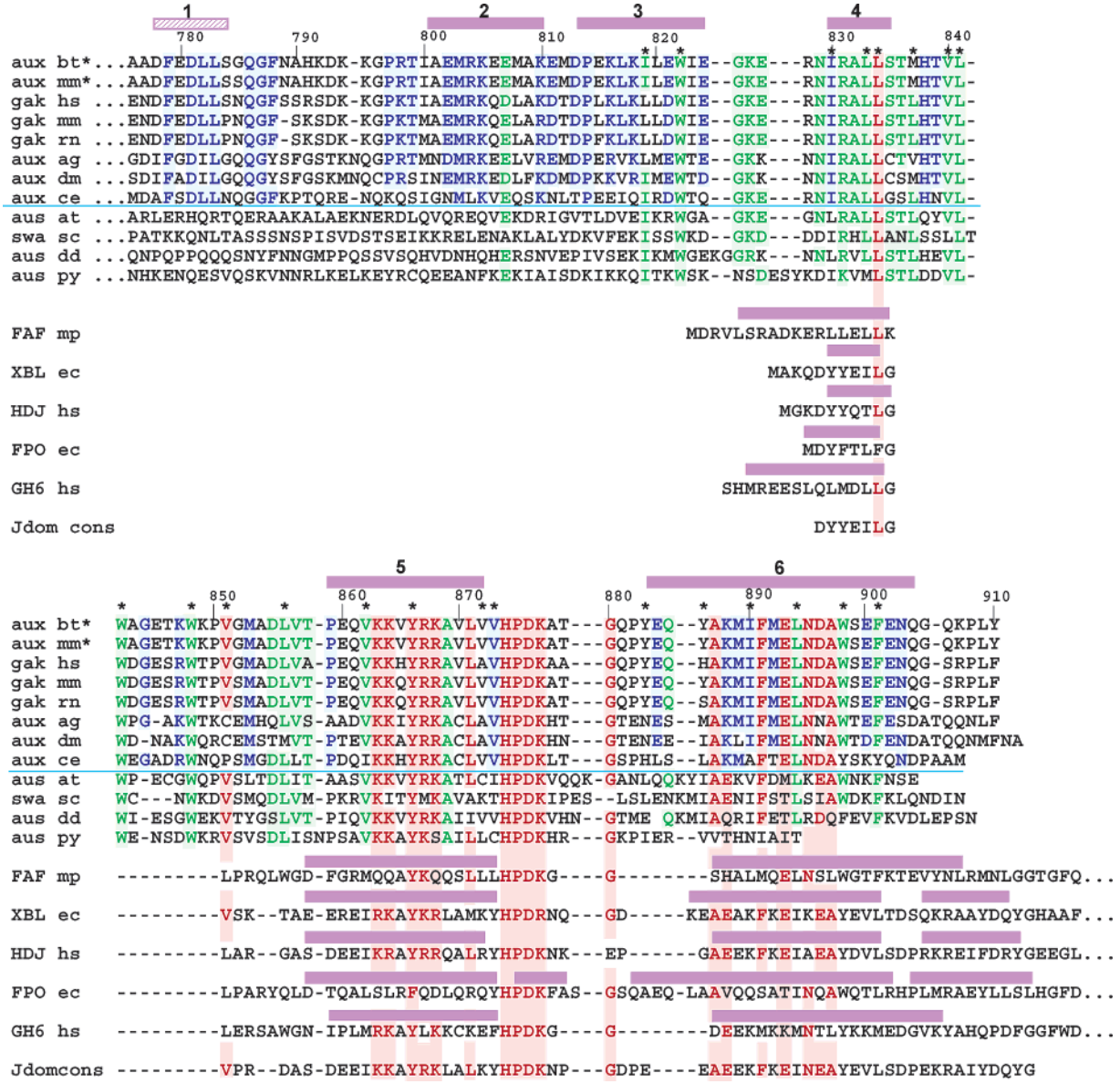

FIGURE 2: Sequence comparison of the auxilin family in eukaryotic phyla and secondary structure comparison with other J-domain proteins. Purple bars represent helices. Asterisks denote hydrophobic core residues. Red highlighting denotes residues conserved in all J-domains, green residues conserved in the auxilin family, and blue conserved residues specific to the animal branch of the auxilin family. Helix 1 of Aux-C20 is transiently structured. The top seven sequences, separated from the rest by the blue line, are animal auxilin sequences. For this region of auxilin, the *Bos taurus* and human sequences are identical, and the *Mus musculus* and *Rattus norvegicus* sequences are identical. For comparison, plant, fungi, amoeba, and plasmodia auxilin-like sequences are shown. Abbreviations: aux, auxilin; gak, cyclin G-associated kinase; aus, similar to aux; swa, similar to yeast swa2; FAF, murine polyomavirus T antigen; XBL, *E. coli* DnaJ; HDJ, *Homo sapiens* DnaJ homologue; FPO, *E. coli* Hsc20; GH6, simian virus 40 large T antigen; bt, *B. taurus*; hs, *H. sapiens*; mm, *M. musculus*; rn, *R. norvigecus*; ag, *Anopheles gambiae*; dm, *Drosophila melanogaster*; ce, *C. elegans*; at, *Arabidopsis thaliana*; sc, *Saccharomyces cerevisiae*; dd, *Dictyostelium discoideum*; py, *Plasmodium yoelli*.

helices pack tightly together, forming the hydrophobic core of the J-domain. An X-ray structure for auxilin, including just the last four helices, matches closely the corresponding portion of the NMR structure with a backbone rms deviation of 1.28 Å (*19*). The extent to which the unbound structure resembles auxilin in its clathrin-bound form of course requires knowledge of the auxilin−clathrin complex structure, which is not known. The FEDLL motif is clearly required since mutation of residues in this motif greatly reduces the activity of Aux-C20 (ref *27* and our unpublished data). However, in addition to the FEDLL motif, the residues preceding helix 1 in the Aux-C20 construct might also be important for clathrin interaction since deleting these residues also greatly reduces activity (*27*), even though these residues are not conserved. Portions of auxilin outside the Aux-C20 construct could also conceivably influence the structure of the flexible regions of Aux-C20, though since Aux-C20 retains catalytic activity, any such influence does not appear to be critical.

Figure 2 compares the sequence of the bovine auxilin J-domain with other auxilin sequences from animals and sequences similar to that of auxilin from plants, fungi, amoeba, and plasmodia. Curiously, in nonanimal auxilin, there do not appear to be any sequence stretches homologous to helix 1 of animal auxilin, and the extent of homology with helix 2 of animal auxilin appears to be marginal, at best. Helix 3 does appear to be conserved in all auxilins, however, because the hydrophobic residues it contributes to

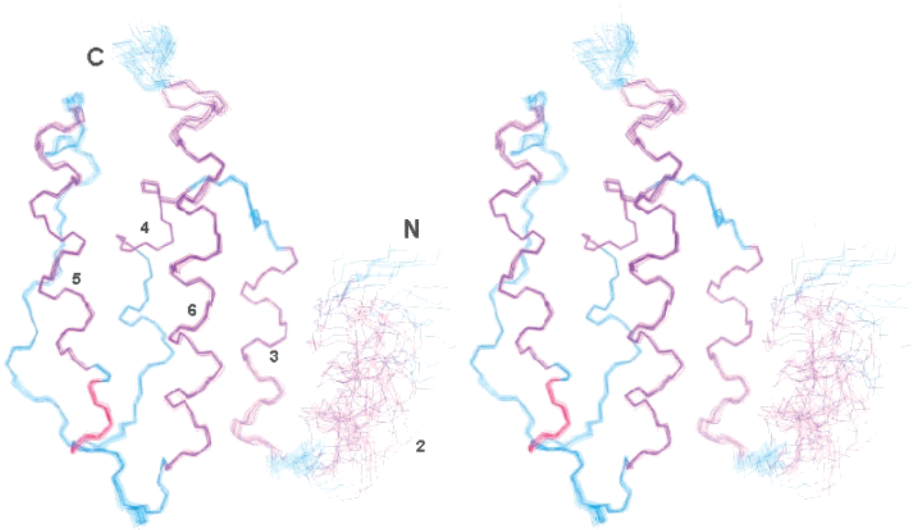

FIGURE 3: Stereoview of the ensemble of 20 NMR structures showing the backbone from the beginning of helix 2 to the C-terminus. Helices are in purple, and the HPD segment is in red. The linker joining helices 1 and 2 is flexible, and the position of helix 1 is not well-determined relative to the rest of the protein.

the J-domain core are found in all auxilin sequences. Also shown in Figure 2 are the sequences and secondary structures of the other five J-domains whose structures have been determined (*20*, *21*, *24*, *41*, *42*). The additional C-terminal helix seen in three of the five other known J-domain structures is not present in the Aux-C20 structure. A Dali structural similarity search (*43*) for Aux-C20 helices 2−6 produced only one non-auxilin match with a score above 5.0, the murine polyomavirus T antigen J-domain [PDB entry 1FAF (*41*)], which happens to be one of the J-domain structures lacking the final C-terminal helix.

Invariant HPD Loop. The structure of the invariant HPD segment is especially interesting because of its critical role in the binding of the J-domain to Hsc70 (*6*, *44*). Surprisingly, the HPD backbone in the Aux-C20 solution structure is not similar to the crystal structure of the auxilin J-domain (HPD backbone rms deviation of 2.7 Å), but it is nearly identical to that seen for Hsc20 [PDB entry 1FPO (*20*); rms deviation of 0.4 Å] and also similar to the murine polyomavirus T antigen J-domain [PDB entry 1FAF (*41*); rms deviation of 1.2 Å]. In fact, the HPD backbone in the auxilin J-domain crystal structure is a bit of an outlier when compared with all other known J-domain structures, being closest to that seen for the human DnaJ homologue [PDB entry 1HDJ (*42*); rms deviation of 1.5 Å].

In the Aux-C20 solution structure, the orientation of the HPD segment histidine ring is accurately determined due to numerous NOE restraints to its side chain. However, in the auxilin J-domain crystal structure, the histidine ring is flipped by 180°. Curiously, the crystal structure of Hsc20 also has the histidine ring flipped 180°, but the large T antigen J-domain (PDB entry 1FAF) has the histidine in the same orientation as the Aux-C20 solution structure. Examination of the other J-domain structures shows that some have the histidine ring like the Aux-C20 solution structure and some closer to the crystal structure of the auxilin J-domain, and some have histidine side chains in still different conformations. While there appears to be no obvious reason for this variety, a clue might come from the structures of the DnaJ J-domain determined both with and without the following G/F-rich domain (*25*). The structure of the HPD segment differed markedly depending on whether the G/F-rich domain was present, even though the G/F-rich domain was unstructured and no direct contact with the HPD loop was observed. Thus, residues outside the J-domain can potentially influence the HPD loop structure. The Aux-C20 construct used for the solution structure has 84 additional N-terminal residues compared to the construct used for the crystal structure. Of course, differing conditions in the crystal compared to those in solution could also give rise to structural differences.

Helix 1 and the Long Insert Loop of Auxilin. The two most distinguishing features of Aux-C20 are its first three helices, the first of which is known to interact with clathrin (27), and its long insert loop between helices 4 and 5 (the first and second helices, respectively, of the canonical J-domains). The J-domain lies at the C-terminus of auxilin, and is the only C-terminal J-domain whose structure is known. Given the large amount of data for the auxilin−clathrin interaction (*7*, *8*, *18*, *26*, *27*), the structure of Aux-C20, including helix 1 with its FEDLL clathrin interacting motif, should provide important insights into the J-domain−substrate interactions in general.

As reported for the X-ray structure of the auxilin J-domain, the long insert loop provides two additional positively charged residues (residues 847 and 849 in Figure 2) to the large positive patch on the auxilin surface and may explain why auxilin, compared with other J-domain proteins, binds much more tightly to Hsc70 (*19*). This patch very likely provides an important part of the interface between the J-domain and its chaperone partner Hsc70 (*44*). It is interesting to note that K847 is conserved for animal auxilins, though not K849, but that neither residue is conserved in nonanimal auxilins (see Figure 2). In fact, the most highly conserved residues of the long insert loop, instead, form part of the hydrophobic core of the auxilin J-domain. In particular, L841, along with M837, forms part of the center of the J-domain hydrophobic core and provides extensive hydrophobic contacts with helix 3, while W848 appears to stabilize the outer part of the loop. Both the long insert loop and helix 3 are unique to the auxilin J-domain; thus, it could be that

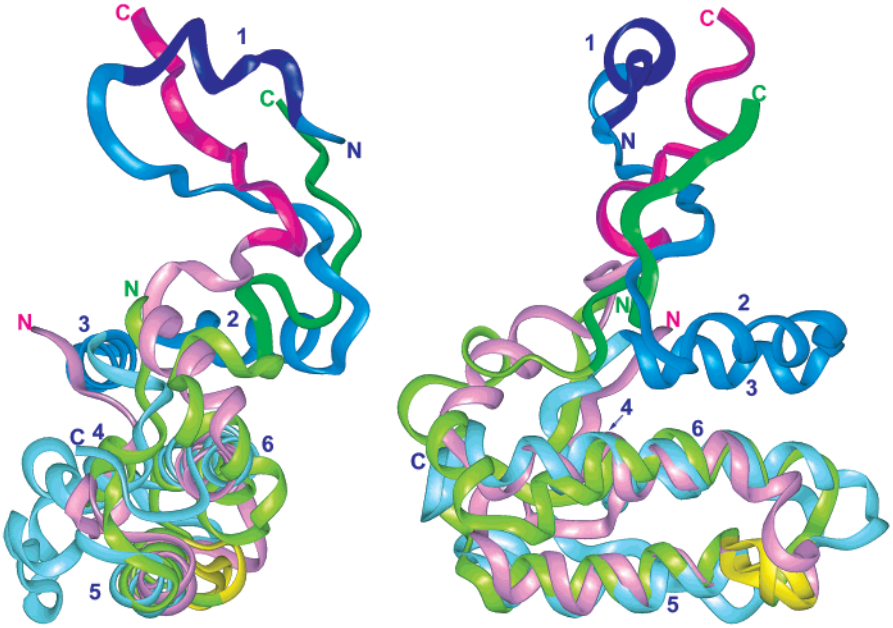

FIGURE 4: Comparison of auxilin with DnaJ and its human homologue. The second view is rotated 90° relative to the first. The Aux-C20 helices are numbered. Aux-C20 helices 4−6 correspond to helices 1−3, respectively, of the canonical J-domain. For the purposes of illustration, the first 10 residues past the C-termini of the DnaJ J-domains, corresponding to the unstructured G/F-rich region, have been appended using random backbone ϕ and ψ angles. Auxilin is blue, with helix 1 darkest blue, and the stretch containing helices 2 and 3 medium blue. *E. coli* DnaJ is green, with dark green showing the appended G/F-rich domain residues, and the human homologue is pink, with dark pink showing the appended residues. The HPD segment for each structure is in yellow.

the more general role of the long insert loop is to provide the hydrophobic core scaffolding for the correct orientation and tight packing of helix 3.

Since helix 2 contacts helices 3 and 6, the correct packing of helix 3 with the J-domain is likely to be important for the positioning of helix 2. Furthermore, modeling of auxilin with its chaperone partner Hsc70 suggests that helix 2 might also contact the substrate binding domain of Hsc70 (J. M. Gruschus *et al*., personal communication). The placement of helix 2 could thus influence the location of the clathrin interacting FEDLL motif of helix 1 with respect to both the J-domain and Hsc70.

Comparison of Helix 1 of Aux-C20 with the Putative Substrate Interacting Regions of Other J-Domains. The positioning of helix 1 of Aux-C20 is compared with the G/F-rich domain of bacterial DnaJ and its human homologue in Figure 4. In DnaJ, the G/F-rich domain, followed by a Zn-finger domain, lies at the C-terminus of DnaJ. DnaJ acts in concert with DnaK (the Hsp70 homologue in *E. coli*) and GrpE as a chaperone system to help fold misfolded or aggregated proteins (*1*). Both the G/F-rich domain and the Zn-finger domain are needed for substrate interaction, and the G/F-rich domain also interacts with DnaK (*45*, *46*). For the purposes of illustration, 10 additional DnaJ residues with random backbone angles have been appended to the C-termini, since the G/F-rich domain is unstructured and, thus, not included in the available structures. Figure 4 shows that helix 1 is in the same general location as the G/F-rich domain, and by extension, the DnaJ Zn-finger domain should not be much further out. This suggests that, despite differences in structure and substrate interactions, there might be similarities in how auxilin and DnaJ present their respective substrates to the substrate binding domains of their Hsp70 partners. However, DnaJ does not have anything structurally analogous to helices 2 and 3, supporting the view that these helices play a specific role in the uncoating of clathrin-coated vesicles catalyzed by auxilin. Large differences between the structure of the G/F-rich region and helices 1−3 of auxilin may explain why most J-domain proteins markedly activate Hsc70 ATPase activity in the absence of substrate, while auxilin only does so in the presence of clathrin baskets (*7*, *28*).

In contrast to DnaJ, comparison of auxilin with the SV40 large T antigen complexed with Rb tumor suppressor shows that the T antigen C-terminal substrate interacting region is not spatially near helix 1 (Figure 5A). In fact, given what is already known about the location of the interaction interface between the J-domain and the Hsc70 ATPase domain (*6*, *44*, *47*, *48*), it would seem that the SV40 large T antigen substrate interacting region and its bound substrate might sterically clash with Hsc70 because the substrate binding region is too close to the HPD loop and preceding helix. The linker between the substrate interacting region and the large T antigen J-domain appears to be flexible, however, so this location of the substrate interacting region could be due to crystal packing. Considerable flexibility is seen in the auxilin, DnaJ, and large T antigen substrate interacting regions; this flexibility might be important for understanding the mechanism of substrate transfer in the Hsp40−Hsp70 chaperone system.

The comparison with the Hsc20 J-domain and C-terminal domain shows the putative interaction region (*20*) of the C-terminal domain in a location distinct from both helix 1 and from the large T antigen substrate interacting regions (Figure 5B). Hsc20 also lacks nearly all of the J-domain positive patch residues (see Figure 2, FPO), hinting at even greater differences in how Hsc20 interacts with its Hsp70 cognate partner Hsc66. Thus, it appears that neither the large T antigens nor Hsc20 interacts with their substrates or presents them to Hsp70 in a manner similar to that of auxilin

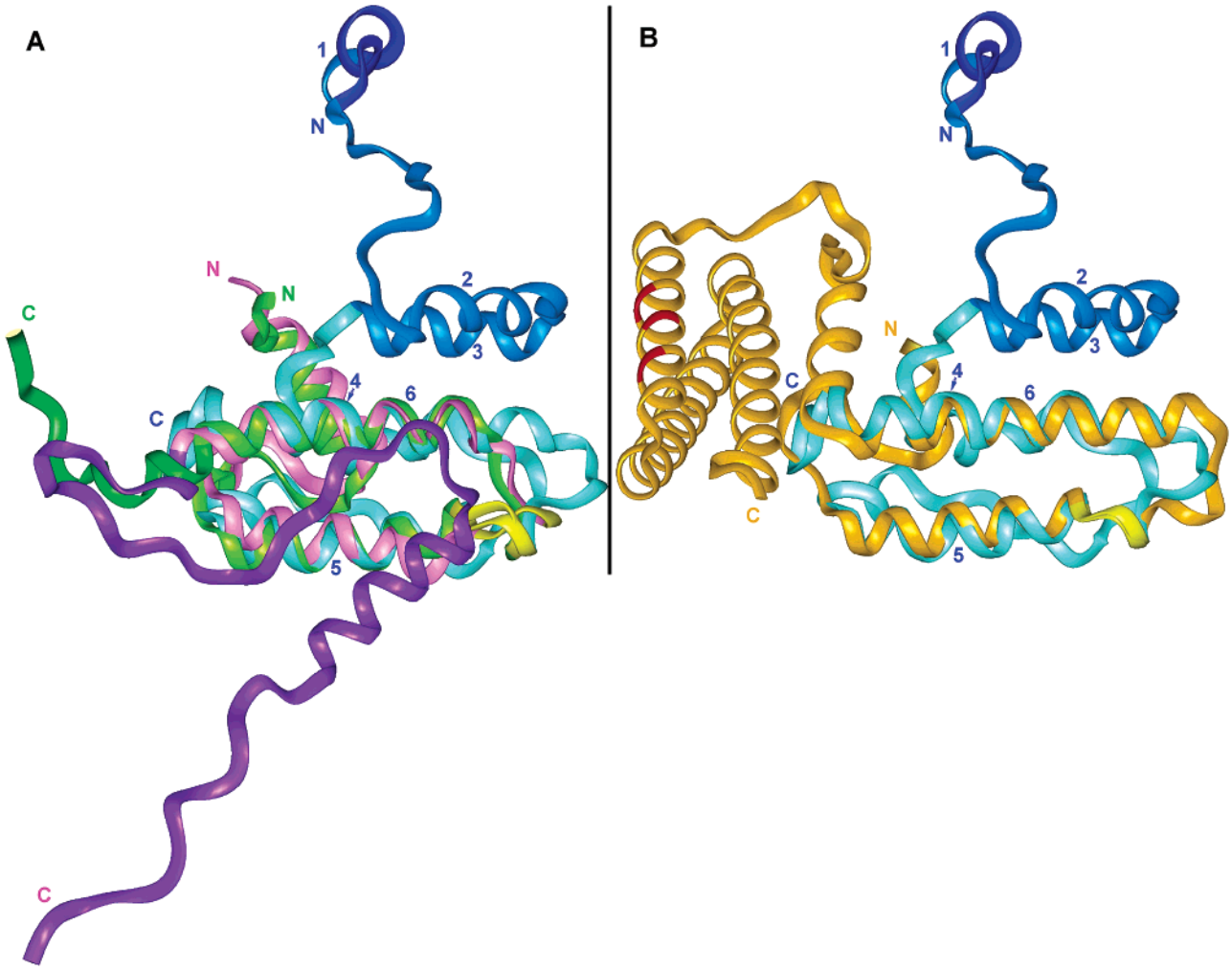

FIGURE 5: Comparison of auxilin with (A) large T antigen J-domains and (B) Hsc20. Auxilin is shown in blue, as in Figure 4. In panel A, the murine polyomavirus J-domain is green, with darker green for the residues past the C-terminus of the J-domain, and the simian virus 40 J-domain is pink, with darker pink for the residues past the J-domain C-terminus. In panel B, Hsc20 is gold, with the conserved acidic residues of its putative interacting region in red. The HPD segments are in yellow.

and DnaJ. Therefore, these results suggest that the specificity in the interaction of Hsc70 with its substrate is conferred by the J-domain protein. The specific J-domain protein recognizes its substrate and then brings it in the correct orientation relative to the Hsc70−ATP molecule so that the substrate can be transferred from the J-domain protein to Hsc70 while at the same time the Hsc70 ATPse activity is activated so that the substrate is trapped on the Hsc70−ADP molecule.

ACKNOWLEDGMENT

We thank Dr. Rodney Levine for performing mass spectroscopy analysis on the Aux-C20 samples.

REFERENCES

1. Mayer, M. P., Rudiger, S., and Bukau, B. (2000) Molecular basis for interactions of the DnaK chaperone with substrates, *Biol. Chem. 381*, 877−885.
2. Greene, L. E., Zinner, R., Naficy, S., and Eisenberg, E. (1995) Effect of nucleotide on the binding of peptides to 70-kDa heat shock protein, *J. Biol. Chem. 270*, 2967−2973.
3. Kelley, W. L. (1998) The J-domain family and the recruitment of chaperone power, *Trends Biochem. Sci. 23*, 222−227.
4. Wall, D., Zylicz, M., and Georgopoulos, C. (1994) The NH_2-Terminal 108 Amino-Acids of the *Escherichia coli* DnaJ Protein Stimulate the ATPase Activity of DnaK and Are Sufficient for Lambda-Replication, *J. Biol. Chem. 269*, 5446−5451.
5. Tsai, J., and Douglas, M. G. (1996) A conserved HPD sequence of the J-domain is necessary for YDJ1 stimulation of Hsp70 ATPase activity at a site distinct from substrate binding, *J. Biol. Chem. 271*, 9347−9354.
6. Suh, W. C., Burkholder, W. F., Lu, C. Z., Zhao, X., Gottesman, M. E., and Gross, C. A. (1998) Interaction of the Hsp70 molecular chaperone, DnaK, with its cochaperone DnaJ, *Proc. Natl. Acad. Sci. U.S.A. 95*, 15223−15228.
7. Barouch, W., Prasad, K., Greene, L., and Eisenberg, E. (1997) Auxilin-induced interaction of the molecular chaperone Hsc70 with clathrin baskets, *Biochemistry 36*, 4303−4308.
8. Ungewickell, E., Ungewickell, H., Holstein, S. E. H., Lindner, R., Prasad, K., Barouch, W., Martin, B., Greene, L. E., and Eisenberg, E. (1995) Role of Auxilin in Uncoating Clathrin-Coated Vesicles, *Nature 378*, 632−635.
9. Greener, T., Zhao, X. H., Nojima, H., Eisenberg, E., and Greene, L. E. (2000) Role of cyclin G-associated kinase in uncoating clathrin-coated vesicles from non-neuronal cells, *J. Biol. Chem. 275*, 1365−1370.
10. Umeda, A., Meyerholz, A., and Ungewickell, E. (2000) Identification of the universal cofactor (auxilin 2) in clathrin coat dissociation, *Eur. J. Cell Biol. 79*, 336−342.
11. Pishvaee, B., Costaguta, G., Yeung, B. G., Ryazantsev, S., Greener, T., Greene, L. E., Eisenberg, E., McCaffery, J. M., and Payne, G. S. (2000) A yeast DNA J protein required for uncoating of clathrin-coated vesicles in vivo, *Nat. Cell Biol. 2*, 958−963.
12. Gall, W. E., Higginbotham, M. A., Chen, C. Y., Ingram, M. F., Cyr, D. M., and Graham, T. R. (2000) The auxilin-like phosphoprotein Swa2p is required for clathrin function in yeast, *Curr. Biol. 10*, 1349−1358.

13. Greener, T., Grant, B., Zhang, Y. H., Wu, X. F., Greene, L. E., Hirsh, D., and Eisenberg, E. (2001) *Caenorhabditis elegans* auxilin: a J-domain protein essential for clathrin-mediated endocytosis in vivo, *Nat. Cell Biol. 3*, 215−219.
14. Ahle, S., and Ungewickell, E. (1990) Auxilin, A Newly Identified Clathrin-Associated Protein in Coated Vesicles from Bovine Brain, *J. Cell Biol. 111*, 19−29.
15. Greene, L. E., and Eisenberg, E. (1990) Dissociation of Clathrin from Coated Vesicles by the Uncoating ATPase, *J. Biol. Chem. 265*, 6682−6687.
16. Jiang, R., Gao, B., Prasad, K., Greene, L. E., and Eisenberg, E. (2000) Hsc70 chaperones clathrin and primes it to interact with vesicle membranes, *J. Biol. Chem. 275*, 8439−8447.
17. Jiang, R. F., Greener, T., Barouch, W., Greene, L., and Eisenberg, E. (1997) Interaction of auxilin with the molecular chaperone, Hsc70, *J. Biol. Chem. 272*, 6141−6145.
18. Ma, Y. C., Greener, T., Pacold, M. E., Kaushal, S., Greene, L. E., and Eisenberg, E. (2002) Identification of domain required for catalytic activity of auxilin in supporting clathrin uncoating by Hsc70, *J. Biol. Chem. 277*, 49267−49274.
19. Jiang, J. W., Taylor, A. B., Prasad, K., Ishikawa-Brush, Y., Hart, P. J., Lafer, E. M., and Sousa, R. (2003) Structure−function analysis of the auxilin J-domain reveals an extended Hsc70 interaction interface, *Biochemistry 42*, 5748−5753.
20. Cupp-Vickery, J. R., and Vickery, L. E. (2000) Crystal structure of Hsc20, a J-type co-chaperone from *Escherichia coli*, *J. Mol. Biol. 304*, 835−845.
21. Kim, H. Y., Ahn, B. Y., and Cho, Y. (2001) Structural basis for the inactivation of retinoblastoma tumor suppressor by SV40 large T antigen, *EMBO J. 20*, 295−304.
22. Szyperski, T., Pellecchia, M., Wall, D., Georgopoulos, C., and Wuthrich, K. (1994) NMR Structure Determination of the *Escherichia coli* DnaJ Molecular Chaperone: Secondary Structure and Backbone Fold of the N-Terminal Region (Residues 2−108) Containing the Highly Conserved J-Domain, *Proc. Natl. Acad. Sci. U.S.A. 91*, 11343−11347.
23. Hill, R. B., Flanagan, J. M., and Prestegard, J. H. (1995) ^{1}H and ^{15}N Magnetic Resonance Assignments, Secondary Structure, and Tertiary Fold of *Escherichia coli* DnaJ(1−78), *Biochemistry 34*, 5587−5596.
24. Pellecchia, M., Szyperski, T., Wall, D., Georgopoulos, C., and Wuthrich, K. (1996) NMR structure of the J-domain and the Gly/Phe-rich region of the *Escherichia coli* DnaJ chaperone, *J. Mol. Biol. 260*, 236−250.
25. Huang, K., Flanagan, J. M., and Prestegard, J. H. (1999) The influence of C-terminal extension on the structure of the "J-domain" in *E. coli* DnaJ, *Protein Sci. 8*, 203−214.
26. Scheele, U., Kalthoff, C., and Ungewickell, E. (2001) Multiple interactions of auxilin 1 with clathrin and the AP-2 adaptor complex, *J. Biol. Chem. 276*, 36131−36138.
27. Scheele, U., Alves, R., Frank, R., Duwel, M., Kalthoff, C., and Ungewickell, E. (2003) Molecular and functional characterization of clathrin- and AP-2-binding determinants within a disordered domain of auxilin, *J. Biol. Chem. 278*, 25357−25368.
28. King, C., Eisenberg, E., and Greene, L. E. (1999) Interaction between Hsc70 and DnaJ homologues: Relationship between Hsc70 polymerization and ATPase activity, *Biochemistry 38*, 12452−12459.
29. Grzesiek, S., and Bax, A. (1993) Amino-Acid Type Determination in the Sequential Assignment Procedure of Uniformly C-13/N-15-Enriched Proteins, *J. Biomol. NMR 3*, 185−204.
30. Vuister, G. W., and Bax, A. (1992) Resolution Enhancement and Spectral Editing of Uniformly C-13-Enriched Proteins by Homonuclear Broad-Band C-13 Decoupling, *J. Magn. Reson. 98*, 428−435.
31. Grzesiek, S., and Bax, A. (1993) The Importance of Not Saturating H_2O in Protein NMR: Application to Sensitivity Enhancement and NOE Measurements, *J. Am. Chem. Soc. 115*, 12593−12594.
32. Muhandiram, D. R., and Kay, L. E. (1994) Gradient-Enhanced Triple-Resonance Three-Dimensional NMR Experiments with Improved Sensitivity, *J. Magn. Reson., Ser. B 103*, 203−216.
33. Gruschus, J. M., and Ferretti, J. A. (1999) Signal enhancement using 45 degrees water flipback for 3D N-15-edited ROESY and NOESY HMQC and HSQC, *J. Magn. Reson. 140*, 451−459.
34. Piotto, M., Saudek, V., and Sklenar, V. (1992) Gradient-Tailored Excitation for Single-Quantum NMR Spectroscopy of Aqueous Solutions, *J. Biomol. NMR 2*, 661−665.
35. Han, C. J., Gruschus, J. M., Greener, T., Greene, L. E., Ferretti, J., and Eisenberg, E. (2000) H-1, N-15, and C-13 NMR backbone assignments and secondary structure of the C-terminal recombinant fragment of auxilin including the J-domain, *J. Biomol. NMR 17*, 281−282.
36. Gruschus, J. M., Tsao, D. H. H., Wang, L. H., Nirenberg, M., and Ferretti, J. A. (1999) The three-dimensional structure of the vnd/NK-2 Homeodomain-DNA complex by NMR spectroscopy, *J. Mol. Biol. 289*, 529−545.
37. Guntert, P., Braun, W., and Wuthrich, K. (1991) Efficient Computation of Three-Dimensional Protein Structures in Solution from Nuclear Magnetic Resonance Data Using the Program DIANA and the Supporting Programs CALIBA, HABAS and GLOMSA, *J. Mol. Biol. 217*, 517−530.
38. Cornilescu, G., Delaglio, F., and Bax, A. (1999) Protein backbone angle restraints from searching a database for chemical shift and sequence homology, *J. Biomol. NMR 13*, 289−302.
39. Folmer, R. H. A., Hilbers, C. W., Konings, R. N. H., and Nilges, M. (1997) Floating stereospecific assignment revisited: Application to an 18 kDa protein and comparison with J-coupling data, *J. Biomol. NMR 9*, 245−258.
40. Sari, N., Alexander, P., Bryan, P. N., and Orban, J. (2000) Structure and dynamics of an acid-denatured protein G mutant, *Biochemistry 39*, 965−977.
41. Berjanskii, M. V., Riley, M. I., Xie, A. Y., Semenchenko, V., Folk, W. R., and Van Doren, S. R. (2000) NMR structure of the N-terminal J domain of murine polyomavirus T antigens: Implications for DnaJ-like domains and for mutations of T antigens, *J. Biol. Chem. 275*, 36094−36103.
42. Qian, Y. Q., Patel, D., Hartl, F. U., and Mccoll, D. J. (1996) Nuclear magnetic resonance solution structure of the human Hsp40 (HDJ-1) J-domain, *J. Mol. Biol. 260*, 224−235.
43. Holm, L., and Sander, C. (1993) Protein-Structure Comparison by Alignment of Distance Matrices, *J. Mol. Biol. 233*, 123−138.
44. Greene, M. K., Maskos, K., and Landry, S. J. (1998) Role of the J-domain in the cooperation of Hsp40 with Hsp70, *Proc. Natl. Acad. Sci. U.S.A. 95*, 6108−6113.
45. Karzai, A. W., and McMacken, R. (1996) A bipartite signaling mechanism involved in DnaJ-mediated activation of the *Escherichia coli* DnaK protein, *J. Biol. Chem. 271*, 11236−11246.
46. Szabo, A., Korszun, R., Hartl, F. U., and Flanagan, J. (1996) A zinc finger-like domain of the molecular chaperone DnaJ is involved in binding to denatured protein substrates, *EMBO J. 15*, 408−417.
47. Gassler, C. S., Buchberger, A., Laufen, T., Mayer, M. P., Schroder, H., Valencia, A., and Bukau, B. (1998) Mutations in the DnaK chaperone affecting interaction with the DnaJ cochaperone, *Proc. Natl. Acad. Sci. U.S.A. 95*, 15229−15234.
48. Genevaux, P., Schwager, F., Georgopoulos, C., and Kelley, W. L. (2002) Scanning mutagenesis identifies amino acid residues essential for the in vivo activity of the *Escherichia coli* DnaJ (Hsp40) J-domain, *Genetics 162*, 1045−1053.
49. Ikura, M., Kay, L. E., Tschudin, R., and Bax, A. (1990) Three-dimensional NOESY HSQC spectroscopy of a C-13 labeled protein, *J. Magn. Reson. 86*, 204−209.
50. Marion, D., Driscoll, P. C., Kay, L. E., Windfield, P. T., Bax, A., Gronenborn, A., and Clore, M. (1989) Overcoming the overlap problem in the assignment of proton NMR spectra of larger proteins by use of three-dimensional heteronuclear ^{1}H−^{15}N Hartmann−Hahn−multiple quantum coherence and nuclear Overhauser−multiple quantum coherence spectroscopy: application to interleukin 1β, *Biochemistry 28*, 6150−6156.

BI0354740